Nanoscale

COMMUNICATION

View Article Online
View Journal | View Issue

Nanostructures on graphene using supramolecule and supramolecular nanocomposites†

Cite this: *Nanoscale*, 2014, **6**, 4503

Received 22nd January 2014
Accepted 5th March 2014

DOI: 10.1039/c4nr00420e

www.rsc.org/nanoscale

Peter Bai,[a] Joseph Kao,[a] Jian-Hao Chen,‡[b] William Mickelson,[b] Alex Zettl[bc] and Ting Xu*[acd]

Nanopatterning and functionalizing of graphene is often required to tune or enhance its unique physical properties. However, complex processes are needed to overcome the chemical incompatibilities between the patterning template, the functional small molecules or nanoparticles, and the underlying graphene. We present a block copolymer (BCP)-based supramolecular thin film as a versatile platform for the generation of periodic patterns of small molecules and ordered assemblies of nanoparticles on top of a graphene substrate without chemical modification of any components. The present approach opens opportunities to readily pattern and functionalize graphene, and to investigate the structure–property correlations of graphene/nanoparticle and graphene/small molecule composite materials.

Graphene, a single layer of sp^2 bonded, hexagonally packed carbon atoms, has become a promising material for applications in electronics,[1] sensing,[2] catalysis,[3,4] photovoltaics[5,6] and nanocomposites[7] due to its unique electrical[8,9] and mechanical properties.[10] Graphene can be nanostructured or decorated with small molecules or nanoparticles (NPs) to tune its optical/electronic properties or introduce new functionalities.[11] Graphene nanodots,[12] nano-ribbon[13] and nanomesh[14,15] have been shown to have semiconducting properties not observed in unpatterned graphene sheets, which demonstrate semimetallic behaviour at room temperature. Typically, the patterning process requires an additional step of depositing a grafting layer, such as polydopamine[16] or SiO_2,[14] on top of graphene or a chemical modification step[17] to increase its surface energy and prevent the dewetting of the sacrificial layer. Furthermore, the graphene surface energy must be precisely tailored to balance the polymer/surface interfacial interactions to control the macroscopic orientation of BCP microdomains. Decoration of graphene by small molecules is a common route to tune its bandgap or increase its chemical reactivity, which increases its competitive strength in the field of semiconductors and sensors.[11] Graphene surfaces decorated with metal or semiconducting NPs act as efficient sensing, catalytic or photovoltaic device components in which the graphene acts as a conductive layer to deliver electrical charges across the device.[3,5,18–22] The NPs can be placed onto the graphene surface *via in situ* reduction of precursors, which requires different synthetic chemistries for different types of NPs,[23–26] or *via* adsorption of preformed NPs to the graphene surface, which requires chemical modification of the graphene or NP surface.[27,28] These modifications may affect the physical properties of the graphene and NPs. In addition, these approaches often cannot guarantee a desired spatial distribution of NPs on the graphene, which is important to generate reliable devices.

We present a simple, versatile approach to nanoscopically pattern graphene using BCP-based supramolecules and decorate graphene with small molecules or NPs without the need to modify the graphene surface, small molecule or NP chemistry as required in many previous studies. The supramolecule, comprised of a BCP hydrogen bonded with small molecules, has three main advantages to modify graphene surface in comparison to prior approaches with conventional BCP systems. Firstly, small molecules situated close to the supramolecule/graphene interface can mediate the interfacial interaction energy,[29] thus allowing for the generation of perpendicular nanostructures and preventing the supramolecule thin film from dewetting on top of the low surface energy graphene, which is commonly observed for other BCP systems.[15,16] Secondly, the non-covalently bonded small molecules can be removed *via* a selective solvent,[30–32] thus generating an etching

[a]*Department of Materials Science and Engineering, University of California, Berkeley, Berkeley, CA, USA. E-mail: tingxu@berkeley.edu*

[b]*Department of Physics, Univeristy of California, Berkeley, Berkeley, CA, USA*

[c]*Materials Sciences Division, Lawrence Berkeley National Laboratory, 1 Cyclotron Road, Berkeley, CA, USA*

[d]*Department of Chemistry, Univeristy of California, Berkeley, Berkeley, CA, USA*

† Electronic supplementary information (ESI) available: Experimental details and GISAXS characterization of supramolecular nanocomposite thin films on graphene substrate. See DOI: 10.1039/c4nr00420e

‡ Current address: International Center for Quantum Materials, Peking University, 6th Floor, Science Building 5, No. 5 Yiheyuan Road, Haidian District, Beijing, 100871, China.

mask to pattern the underlying graphene. Additional functionalities can be readily introduced to the graphene surface by exchanging the small molecules with liquid crystalline,[33] semiconducting,[34] or external field[35–37] responsive small molecules. Thirdly, the small molecule can be selected to interact favorably with the NP ligands and leads to the incorporation of NPs into one BCP microdomain.[38–40] This enables the supramolecule to serve as a structure-directing scaffold for the self-assembly of NPs into 1-D arrays and 3-D networks on top of graphene over arbitrarily large areas. Thus, the supramolecular approach greatly simplifies the patterning and functionalization of graphene, and opens opportunities to explore the structure–property correlations of patterned graphene, graphene/small molecule, and graphene/NP nanocomposites.

The supramolecule is comprised of polystyrene-*block*-poly(4-vinylpyridine) (PS-*b*-P4VP) with the P4VP block hydrogen bonded to a small molecule, as shown in Fig. 1a. The supramolecule is denoted as PS(x)-*b*-P4VP(y)(SM)$_n$, where x and y represent the molar weight of the PS and P4VP blocks respectively in units of g mol^{-1}, SM represents the name of the small molecule, and the subscript n represents the molar ratio of small molecule to P4VP. An alkylated small molecule, 3-pentadecylphenol (PDP), is readily incorporated into the block copolymer to form the supramolecule PS-*b*-P4VP(PDP). Fig. 1b shows the AFM and optical microscopy image (inset) of graphene supported on a SiO_2/Si substrate, showing a smooth, uniform coverage of graphene. A thin film of PS(19 000)-*b*-P4VP(5200)(PDP)$_{1.7}$ was spun cast onto the graphene layer and solvent annealed, forming a microphase separated morphology with no signs of dewetting (Fig. 1c). The corresponding optical microscopy image shows a color change due to light interference effects from the thin film. Since the color change is dependent on film thickness, the uniformity of the color change indicates that a smooth supramolecule film is formed on graphene over large areas. A film thickness of 61 nm is measured by interferometry (ESI 1†).

Ordered nanostructure with reasonable long range order is generated by solvent annealing a ~30 nm thin film of PS(19 000)-*b*-P4VP(5200)(PDP)$_{1.7}$ supramolecule *via* exposure to 300 μL of chloroform for 15 min as described in the Experimental details (ESI 2†). With a P4VP(PDP) volume fraction of 0.62, cylindrical morphology was observed with the PS cylinders embedded in the P4VP(PDP) matrix and oriented parallel to the underlying graphene surface. The PS cylinders form a fingerprint-like pattern with a periodicity of ~25 nm (Fig. 2a). Control of microdomain orientation in BCP thin films over macroscopic distances, especially to obtain vertical alignment of microdomain, is challenging because it requires balances between the film/substrate and interfacial interactions [41,42] In the supramolecule thin film, macroscopic alignment of BCP microdomains can be readily tailored by varying the solvent annealing conditions. A thin film of PS(24 000)-*b*-P4VP(9500)(PDP)$_2$, with P4VP(PDP) volume fraction of 0.70, was solvent annealed at a lower vapor pressure with 200 μL chloroform for 12 minutes. This is an optimal annealing condition to stabilize perpendicular cylinder morphology, which can be clearly seen from AFM (Fig. 2b). PDP can be selectively removed from the film by rinsing with isopropyl alcohol[43] to generate line and dot patterns (Fig. 2c and d). The removal of PDP causes a large volumetric shrinkage of the P4VP(PDP) microdomain, which results in a thickness contrast between the PS and P4VP microdomains. These nanopatterned films can potentially be used as sacrificial masks for plasma etching to pattern graphene.

The BCP supramolecule construct enables the formation of perpendicular BCP morphologies and prevents the dewetting of

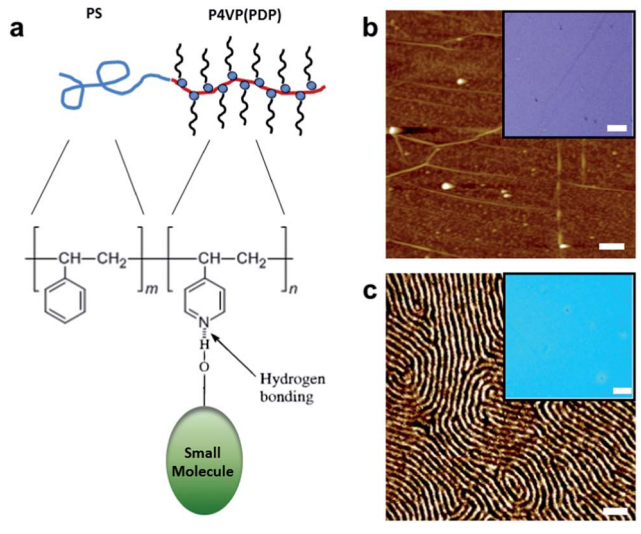

Fig. 1 (a) Schematic of the PS-*b*-P4VP(SM) supramolecule construct. AFM and optical microscope (inset) images of a graphene coated Si substrate (b) before and (c) after being coated with a ~100 nm PS-*b*-P4VP(PDP) supramolecule thin film. Scale bars are 200 nm for the AFM images and 10 μm for the optical microscope images.

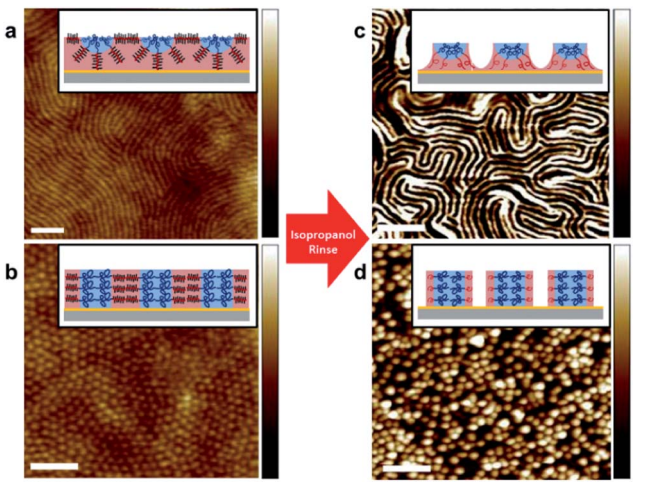

Fig. 2 AFM height images of solvent annealed thin films of (a) PS(19 000)-*b*-P4VP(5200)(PDP)$_{1.7}$ and (b) PS(24 000)-*b*-P4VP(9500)(PDP)$_2$ supramolecules showing cylindrical morphology oriented parallel and perpendicular to the substrate, respectively. After solvent wash with isopropyl alcohol to remove PDP, thin films with parallel cylindrical morphology formed line patterns (c) and thin films with perpendicular cylindrical morphology formed dot patterns (d) with increased height contrast between the microdomains. The scale bars are 200 nm and color scales are 0–20 nm for all images.

the BCP thin film on top of graphene, a phenomenon frequently observed due to the low surface energy of graphene.[15,16] The PDP small molecules in the supramolecule likely play an important role in mediating the graphene/supramolecule interfacial interactions. Grazing Incidence Small Angle X-ray Scattering (GISAXS) is used to investigate the spatial distribution of PDP small molecules within the thin film (ESI 3†). For both parallel and perpendicular cylindrical thin films, there exist a scattering peak at $q_y = 0.155$ Å^{-1} signifying perpendicularly oriented PDP at the graphene/film interface. These PDP molecules could in effect form a brush layer to mediate the graphene/film interfacial interaction. This interfacial energy mediation is the underlying reason that dewetting is not observed with the BCP supramolecule thin film. This PDP-rich layer was also observed in previous studies of supramolecular thin film assembly on a hydrophobic PS-coated substrate.[29] The presence of this PDP-rich brush layer thus serves as a built-in regulator of interfacial interaction that enables thin film and perpendicular morphology formation on the low surface energy graphene.

Another advantage of the supramolecular approach is that the side chain functionalities are readily modular since PDP can be replaced by other small molecules with hydrogen bond donor moieties. This allows semiconducting,[34] liquid crystalline[44] and external field-responsive[36,45,46] small molecules to be incorporated onto a graphene surface. As an example, a photoresponsive azobenzene-containing small molecule, 4-(4′-butylphenyl diazenyl)phenol (4PAP) can be incorporated into the supramolecule (Fig. 3a). Fig. 3b shows the GISAXS scattering of a PS(20 000)-*b*-P4VP(19 000)(4PAP)$_1$ supramolecule thin film annealed in 200 μL chloroform for 12 minutes. A q_y linecut of the GISAXS pattern (inset) shows the $1 : \sqrt{3} : \sqrt{7}$ peak ratios characteristic of perpendicularly oriented cylinders. A broader peak around $q_y = 0.17$ Å^{-1} corresponds to 4PAP scattering. This scattering peak is limited in the q_y direction, suggesting that the 4PAP molecules are highly oriented. Fig. 3c shows the GISAXS scattering and q_y linecut (inset) of a PS(24 000)-*b*-P4VP(9500)(4PAP)$_2$ supramolecule thin film annealed in 300 μL chloroform for 15 min. The 4PAP scattering peak forms a ring instead of being confined in the q_y direction, suggesting random orientation of the 4PAP small molecules. The thin film morphologies are further investigated *via* AFM, which clearly shows the formation of perpendicular cylindrical morphology for the PS(20 000)-*b*-P4VP(19 000)(4PAP)$_1$ supramolecule (Fig. 3d and e) and parallel cylindrical morphology for the PS(24 000)-*b*-P4VP(9500)(4PAP)$_2$ supramolecule (Fig. 3f and g). The close proximity and controllable orientation of 4PAP with respect to graphene may enable tunable electronic coupling between the 4PAP and graphene, which could lead to applications in photoswitching.[47] In addition, azobenezene-containing block copolymers are known to undergo mechanical deformations upon UV light exposure due to the *cis–trans* isomerization of the azobenzene moiety,[37] thus the thin films can potentially

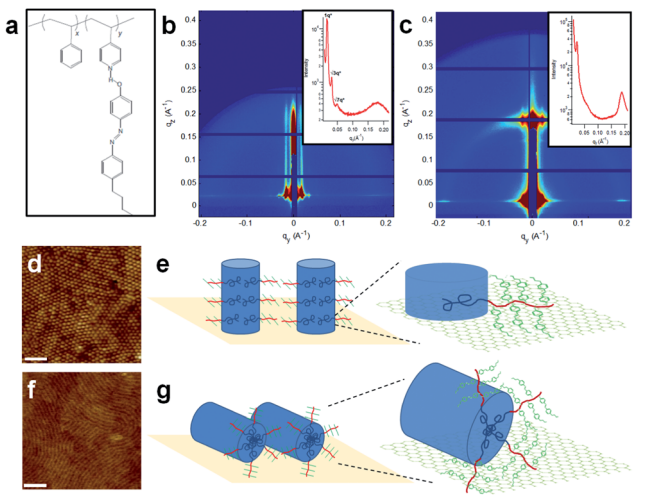

Fig. 3 (a) Schematic of the azobenzene containing supramolecule PS-*b*-P4VP(4PAP). 2D GISAXS pattern and 1D linecut (inset) of PS-*b*-P4VP(4PAP) with (b) PS(20 000)-*b*-P4VP(19 000)(4PAP)$_1$ and (c) PS(24 000)-*b*-P4VP(9500)(4PAP)$_2$ supramolecule thin films on graphene, suggesting perpendicular cylinders with 4PAP molecules aligned parallel to graphene for the PS(20 000)-*b*-P4VP(19 000)(4PAP)$_1$ supramolecule, and parallel cylinders with 4PAP molecules aligned randomly to graphene for the PS(24 000)-*b*-P4VP(9500)(4PAP)$_2$ supramolecule. The thin film morphologies are confirmed *via* AFM and schematically illustrated for the perpendicular (d and e) and parallel (f and g) cylindrical morphologies, detailing the orientation of the BCP cylinders and the 4PAP small molecules relative to the graphene substrate. Scale bars are 200 nm.

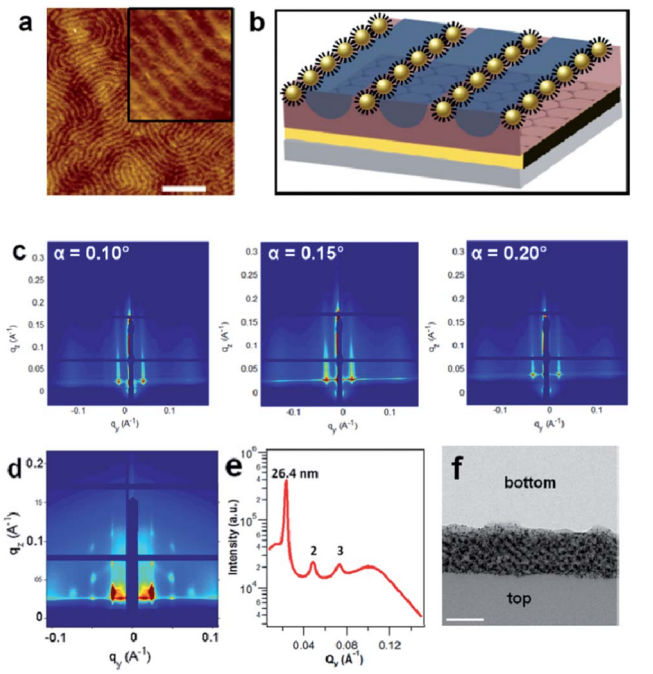

Fig. 4 (a) AFM image and (b) schematic of a solvent annealed PS-*b*-P4VP(PDP)/Au NP nanocomposite thin film self-assembled into parallel line patterns. (c) GISAXS at incidence angles of 0.10°, 0.15° and 0.20° all show strong Bragg rods at $q_y = 0.021$ Å^{-1} and no peaks along the q_z direction, suggesting a monolayer of NP arrays with 30 nm inter-array spacing. For a ~180 nm thick film, the GISAXS pattern (d) shows a scattering pattern characteristic of a hexagonal lattice of NP arrays. A q_y linecut (e) reveals lateral periodicity of ~26 nm with up to third order scattering peak visible. A cross-sectional TEM image (f) of the film shows the Au NP arrays arranged into hexagonal networks as predicted by GISAXS. Scale bars are 200 nm.

be used to mechanically strain graphene and engineer its electronic properties.[48]

The supramolecular thin film also serves as a versatile framework to generate ordered arrays of NPs on graphene. NPs with alkyl ligands interact favorably with the PDP alkyl tails, and can be selectively incorporated into the P4VP(PDP) microdomain of the supramolecular framework. Fig. 4 shows the AFM and GISAXS of a ~30 nm thin film comprised of PS(19 000)-*b*-P4VP(5200)$(PDP)_{1.7}$ and 6 v% of ~4 nm Au NPs covered with dodecanethiol ligands on graphene. The NPs are observed to assemble into 1-D arrays along the darker P4VP(PDP) microdomain (Fig. 4a and b). GISAXS patterns of the film at different incidence angles of $\alpha = 0.10°$, 0.15° and 0.20° (Fig. 4c) all show strong Bragg rods, suggesting a single layer of NPs on top of graphene. 3-D networks of NPs can be generated by increasing the thickness of the nanocomposite film. A ~180 nm film shows a GISAXS pattern with distinctive scattering peaks in the q_y and q_z directions with q_y peak ratios of 1 : 2 : 3 (Fig. 4d and e), characteristic of a distorted hexagonal lattice of parallel oriented NP arrays. The cross-sectional TEM (Fig. 4f) confirms the formation of 3-D NP arrays organized into hexagonal networks on graphene, consistent with GISAXS. Besides Au NPs, previous studies have demonstrated the supramolecule-guided assembly of PbS and PbSe NPs,[39] and CdSe nanorods[49] covered by the common alkyl native ligands. These assemblies can be readily adapted to a graphene substrate, thus establishing the versatility of this supramolecule to decorate graphene with ordered assemblies of functional NPs.

Conclusions

In summary, we have demonstrated BCP-based supramolecular thin films as a versatile platform to pattern and functionalize graphene with several advantages over existing approaches. The interfacial energy mediation provided by the small molecules prevents film dewetting and enables the formation of thin films with both parallel and perpendicular cylindrical nanostructures on the graphene surface. The small molecules can be selectively removed to potentially generate etching masks to pattern the underlying graphene, or replaced with other small molecules to introduce additional functionalities. Incorporation of NPs into this supramolecular nanostructure resulted in 1-D NP arrays and 3-D NP networks on top of graphene. This approach does not require modification of the NP, small molecule or graphene surface chemistries, thus circumventing complex chemical modification steps as required by previous processing methodologies. The decoration of graphene with patterned functional small molecules or ordered NP assemblies may open exciting opportunities to investigate the structure–property correlations underlying NP/graphene and small molecule/graphene nanocomposites. These properties would find numerous applications such as solar cells, sensors, and catalysts.

Acknowledgements

This work was supported by the COINS NSF award EEC-0832819. The Advanced Light Source is supported by the Director, Office of Science, Office of Basic Energy Sciences, of the U.S. Department of Energy under Contract DE-AC02-05CH11231.

Notes and references

1 K. S. Novoselov, A. K. Geim, S. V. Morozov, D. Jiang, Y. Zhang, S. V. Dubonos, I. V. Grigorieva and A. A. Firsov, *Science*, 2004, **306**, 666–669.
2 J. D. Fowler, M. J. Allen, V. C. Tung, Y. Yang, R. B. Kaner and B. H. Weiller, *ACS Nano*, 2009, **3**, 301–306.
3 G. M. Scheuermann, L. Rumi, P. Steurer, W. Bannwarth and R. Muelhaupt, *J. Am. Chem. Soc.*, 2009, **131**, 8262–8270.
4 B. Seger and P. V. Kamat, *J. Phys. Chem. C*, 2009, **113**, 7990–7995.
5 L. G. De Arco, Y. Zhang, C. W. Schlenker, K. Ryu, M. E. Thompson and C. Zhou, *ACS Nano*, 2010, **4**, 2865–2873.
6 J. K. Wassei and R. B. Kaner, *Mater. Today*, 2010, **13**, 52–59.
7 B. Z. Jang and A. Zhamu, *J. Mater. Sci.*, 2008, **43**, 5092–5101.
8 M. I. Katsnelson, K. S. Novoselov and A. K. Geim, *Nat. Phys.*, 2006, **2**, 620–625.
9 Y. B. Zhang, Y. W. Tan, H. L. Stormer and P. Kim, *Nature*, 2005, **438**, 201–204.
10 C. Lee, X. Wei, J. W. Kysar and J. Hone, *Science*, 2008, **321**, 385–388.
11 V. Georgakilas, M. Otyepka, A. B. Bourlinos, V. Chandra, N. Kim, K. C. Kemp, P. Hobza, R. Zboril and K. S. Kim, *Chem. Rev.*, 2012, **112**, 6156–6214.
12 L. A. Ponomarenko, F. Schedin, M. I. Katsnelson, R. Yang, E. W. Hill, K. S. Novoselov and A. K. Geim, *Science*, 2008, **320**, 356–358.
13 X. Li, X. Wang, L. Zhang, S. Lee and H. Dai, *Science*, 2008, **319**, 1229–1232.
14 J. Bai, X. Zhong, S. Jiang, Y. Huang and X. Duan, *Nat. Nanotechnol.*, 2010, **5**, 190–194.
15 M. Kim, N. S. Safron, E. Han, M. S. Arnold and P. Gopalan, *Nano Lett.*, 2010, **10**, 1125–1131.
16 B. H. Kim, D. H. Lee, J. Y. Kim, D. O. Shin, H. Y. Jeong, S. Hong, J. M. Yun, C. M. Koo, H. Lee and S. O. Kim, *Adv. Mater.*, 2011, **23**, 5618–5622.
17 B. H. Kim, J. Y. Kim, S.-J. Jeong, J. O. Hwang, D. H. Lee, D. O. Shin, S.-Y. Choi and S. O. Kim, *ACS Nano*, 2010, **4**, 5464–5470.
18 Y. Choi, H. S. Bae, E. Seo, S. Jang, K. H. Park and B.-S. Kim, *J. Mater. Chem.*, 2011, **21**, 15431–15436.
19 L. Cunci, C. V. Rao, C. Velez, Y. Ishikawa and C. R. Cabrera, *Electrocatalysis*, 2013, **4**, 61–69.
20 Y. Li, X. Fan, J. Qi, J. Ji, S. Wang, G. Zhang and F. Zhang, *Mater. Res. Bull.*, 2010, **45**, 1413–1418.
21 Y. Li, X. Fan, J. Qi, J. Ji, S. Wang, G. Zhang and F. Zhang, *Nano Res.*, 2010, **3**, 429–437.
22 Y.-H. Lu, M. Zhou, C. Zhang and Y.-P. Feng, *J. Phys. Chem. C*, 2009, **113**, 20156–20160.
23 G. Goncalves, P. A. A. P. Marques, C. M. Granadeiro, H. I. S. Nogueira, M. K. Singh and J. Gracio, *Chem. Mater.*, 2009, **21**, 4796–4802.

24 S. Mayavan, J.-B. Sim and S.-M. Choi, *J. Mater. Chem.*, 2012, **22**, 6953–6958.
25 S. Guo, D. Wen, Y. Zhai, S. Dong and E. Wang, *ACS Nano*, 2010, **4**, 3959–3968.
26 A. Gutes, B. Hsia, A. Sussman, W. Mickelson, A. Zettl, C. Carraro and R. Maboudian, *Nanoscale*, 2012, **4**, 438–440.
27 P. V. Kamat, *J. Phys. Chem. Lett.*, 2010, **1**, 520–527.
28 W. Lu, Y. Luo, G. Chang and X. Sun, *Biosens. Bioelectron.*, 2011, **26**, 4791–4797.
29 J. Kao, J. Tingsanchali and T. Xu, *Macromolecules*, 2011, **44**, 4392–4400.
30 S.-H. Tung and T. Xu, *Macromolecules*, 2009, **42**, 5761–5765.
31 R. Maki-Ontto, K. de Moel, W. de Odorico, J. Ruokolainen, M. Stamm, G. ten Brinke and O. Ikkala, *Adv. Mater.*, 2001, **13**, 117–121.
32 A. Sidorenko, I. Tokarev, S. Minko and M. Stamm, *J. Am. Chem. Soc.*, 2003, **125**, 12211–12216.
33 J. T. Korhonen, T. Verho, P. Rannou and O. Ikkala, *Macromolecules*, 2010, **43**, 1507–1514.
34 B. J. Rancatore, C. E. Mauldin, J. M. J. Frechet and T. Xu, *Macromolecules*, 2012, **45**, 8292–8299.
35 P. W. Majewski, M. Gopinadhan and C. O. Osuji, *J. Polym. Sci., Part B: Polym. Phys.*, 2012, **50**, 2–8.
36 C. Osuji, P. J. Ferreira, G. P. Mao, C. K. Ober, J. B. Vander Sande and E. L. Thomas, *Macromolecules*, 2004, **37**, 9903–9908.
37 H. Yu and T. Ikeda, *Adv. Mater.*, 2011, **23**, 2149–2180.
38 J. Kao, P. Bai, V. P. Chuang, Z. Jiang, P. Ercius and T. Xu, *Nano Lett.*, 2012, **12**, 2610–2618.
39 J. Kao, P. Bai, J. M. Lucas, A. P. Alivisatos and T. Xu, *J. Am. Chem. Soc.*, 2013, **135**, 1680–1683.
40 Y. Zhao, K. Thorkelsson, A. J. Mastroianni, T. Schilling, J. M. Luther, B. J. Rancatore, K. Matsunaga, H. Jinnai, Y. Wu, D. Poulsen, J. M. J. Frechet, A. P. Alivisatos and T. Xu, *Nat. Mater.*, 2009, **8**, 979–985.
41 E. Huang, S. Pruzinsky, T. P. Russell, J. Mays and C. J. Hawker, *Macromolecules*, 1999, **32**, 5299–5303.
42 E. Huang, T. P. Russell, C. Harrison, P. M. Chaikin, R. A. Register, C. J. Hawker and J. Mays, *Macromolecules*, 1998, **31**, 7641–7650.
43 W.-H. Huang, P.-Y. Chen and S.-H. Tung, *Macromolecules*, 2012, **45**, 1562–1569.
44 P. Bai, M. I. Kim and T. Xu, *Macromolecules*, 2013, **46**, 5531–5537.
45 H. Yu and T. Kobayashi, *Molecules*, 2010, **15**, 570–603.
46 M. Gopinadhan, P. W. Majewski, E. S. Beach and C. O. Osuji, *ACS Macro Lett.*, 2012, **1**, 184–189.
47 X. Zhang, Y. Feng, P. Lv, Y. Shen and W. Feng, *Langmuir*, 2010, **26**, 18508–18511.
48 J.-K. Lee, S. Yamazaki, H. Yun, J. Park, G. P. Kennedy, G.-T. Kim, O. Pietzsch, R. Wiesendanger, S. Lee, S. Hong, U. Dettlaff-Weglikowska and S. Roth, *Nano Lett.*, 2013, **13**, 3494–3500.
49 K. Thorkelsson, A. J. Mastroianni, P. Ercius and T. Xu, *Nano Lett.*, 2013, **12**, 498–504.